American Mineralogist, Volume 94, pages 323–333, 2009

Fukalite: An example of an OD structure with two-dimensional disorder

S. Merlino,[1] E. Bonaccorsi,[1,2,*] A.I. Grabezhev,[3] A.E. Zadov,[4] N.N. Pertsev,[5] and N.V. Chukanov[6]

[1]Dipartimento di Scienze della Terra, University of Pisa, Italy
[2]CNR-Institute for Geosciences and Georesources, Via Moruzzi 1, Pisa, Italy
[3]Institute of Geology and Geochemistry, Ural Branch of Russian Academy of Science, Pochtovyi Lane 7, Ekaterinburg 620151, Russia
[4]"NPP Teplochim" Limited, Dmitrovskoye Highway 71, Moscow 127238, Russia
[5]Institute of Geology of Ore Deposits, Petrography, Mineralogy and Geochemistry, Russian Academy of Science Moscow, Staromonetny Lane 35, Moscow 119017, Russia
[6]Institute of Problems of Chemical Physics, Russian Academy of Science, Chernogolovka, Moscow Region 142432, Russia

Abstract

The real crystal structure of fukalite, $Ca_4Si_2O_6(OH)_2(CO_3)$, was solved by means of the application of order-disorder (OD) theory and was refined through synchrotron radiation diffraction data from a single crystal. The examined sample came from the Gumeshevsk skarn copper porphyry deposit in the Central Urals, Russia. The selected crystal displays diffraction patterns characterized by strong reflections, which pointed to an orthorhombic sub-structure (the "family structure" in the OD terminology), and additional weaker reflections that correspond to a monoclinic real structure.

The refined cell parameters are $a = 7.573(3)$, $b = 23.364(5)$, $c = 11.544(4)$ Å, $\beta = 109.15(1)°$, space group $P2_1/c$. This unit cell corresponds to one of the six possible maximum degree of order (MDO) polytypes, as obtained by applying the OD procedure. The derivation of the six MDO polytypes is presented in the Appendix[1]. The intensity data were collected at the Elettra synchrotron facility (Trieste, Italy); the structure refinement converged to $R = 0.0342$ for 1848 reflections with $I > 2\sigma(I)$ and 0.0352 for all 1958 data.

The structure of fukalite may be described as formed by distinct structural modules: a calcium polyhedral framework, formed by tobermorite-type polyhedral layers alternating along **b** with tilleyite-type zigzag polyhedral layers; silicate chains with repeat every fifth tetrahedron, running along **a** and linked to the calcium polyhedral layers on opposite sides; and finally rows of CO_3 groups parallel to (100) and stacked along **a**.

Keywords: Crystal structure, fukalite, calcium carbonate silicate, OD structure

Introduction

Fukalite was first found at Fuka, Okayama Prefecture, Japan (Henmi et al. 1977), and subsequently at Mihara, in the same Prefecture, and Kushiro, Hiroshima Prefecture. In the three localities, fukalite occurs in spurrite-gehlenite skarns as an alteration product of spurrite. The occurrence, physical and chemical properties, X-ray crystallography, and thermal behavior of the new mineral have been presented by Henmi et al. (1977) and are here briefly reported.

Fukalite crystals from the type locality are white to pale brown, with the measured density 2.770 g/cm^3; they are optically biaxial ($2V = 90°$) and have refractive indices $\alpha = 1.595$, $\beta = 1.605$, and $\gamma = 1.626$. The chemical analyses, carried out on specimens from Fuka and Mihara are in very good agreement with each other and point to the ideal chemical formula $Ca_4Si_2O_6(OH)_2(CO_3)$.

Weissenberg and precession photographs correspond to an orthorhombic cell, with $a = 5.48$, $b = 3.78$, $c = 23.42$ Å and possible space groups $Bm2_1b$, $Bmmb$, $B2mb$.

More recently fukalite has been found in veinlets cutting hydroxylellestadite metasomatic rock at the Gumeshevsk skarn copper porphyry deposit in the Central Urals, Russia (Grabezhev et al. 2004, 2007) and in skarn carbonate xenoliths of the Dovyren layered gabbro-peridotite massif, North Baikal Region, Russia (Zadov and Pertsev 2005).

Gumeshevsk and Dovyren fukalite: Occurrences, physical and chemical data

The Gumeshevsk deposit is well known from the end of 18th century because of its high quality semi-precious malachite and rich copper ores. Fukalite occurs there in a hydroxylellestadite skarn body developed at the contact of a dike-like quartz-diorite intrusion with lime marble. The metasomatic body consists mainly of hydroxylellestadite (~90 vol%) with admixtures of foshagite, andradite, chlorite, tobermorite, calcite, anhydrite, fukalite, and gypsum. Fukalite was found in the core of the exploration bore hole 3871 in two intervals of the hydroxylellestadite skarn body: 530.4–531.9 m and 533.4–534.5 m of depth.

The upper interval containing fukalite consists of a massive light-bluish-gray rock with 1–3 vol% of calcite, fine grains of andradite, flakes and spherulites of light-green chlorite, rare

* E-mail: elena@dst.unipi.it

clinopyroxene prisms, anhydrite, and titanite grains. Fukalite occurs as colorless small flakes disseminated in the rock and as elongated prisms up to 0.1 mm long occurring in microscopic gypsum veinlets and presenting negative elongation. These have negative elongation and parallel extinction. The fukalite here, according to the optical study, has orthorhombic symmetry just as for the specimen of the type locality. Also the unit-cell dimensions, calculated from the X-ray powder-diffraction pattern [a_o = 5.47(1), b_o = 3.784(2), c_o = 23.38(2) Å], are in keeping with orthorhombic symmetry and closely correspond to those reported for the Fuka specimen.

The lower interval containing fukalite consists of hydroxylellestadite with abundant relics of vesuvianite, andradite, veinlets of gypsum, and rare microveins of fukalite, for which preliminary optical observations point to a monoclinic symmetry. Gyrolite and tacharanite are present in association with fukalite. Gypsum occurs in fukalite veinlets mainly as their salbands.

The Dovyren (Ioko-Dovyren) layered massif (Kislov 1998) is remarkable in many aspects (Pertsev et al. 2003), including abundance of different calcium hydrosilicates replacing calc-magnesian skarns after carbonate xenoliths in dunite (Zadov and Pertsev 2005). Fukalite was found there in the core of the bore hole 143 at a depth of about 705 m. The mineral is developed in a zone of spinel-merwinite skarn which has undergone a low-temperature hydrothermal alteration. Fukalite is located in thin (<1 mm) secondary veinlets with symmetric zonation. The inner zone consists of afwillite, whereas the outer ones are composed mainly of X-ray amorphous Mg-hydrosilicate. The latter contains inclusions of randomly oriented fukalite individual needles and clusters. The concentration of fukalite in the Mg-hydrosilicate zones reaches 20 vol%. Hydroxylellestadite fine grains (with 2 wt% Cl) occur in the Mg-hydrosilicate zones, as well. Due to the micrometer-scale size of the fukalite crystals included in the Mg-hydrosilicate matrix, we were unable to perform optical investigations. A comparative study through electron micro-diffraction of fukalite crystals, both from Dovyren and from the lower fukalite-bearing zone from the Gumeshevsk deposit, points to their identity.

TABLE 1. Chemical composition of fukalite samples

		Gumeshevsk		Dovyren	Fuka	Mihara
Ideal formula $Ca_4(Si_2O_6)(CO_3)(OH)_2$		Orthorhombic (1)	Monoclinic (2)	Monoclinic (3)	Orthorhombic*	
SiO_2	29.56	28.41	29.76	30.00	29.02	28.98
TiO_2		–	–	–	–	–
Al_2O_3		–	–	–	0.55	0.27
Fe_2O_3		–	–	–	0.10	0.14
FeO		0.24				
MnO		–	–	–	–	–
MgO		–	–	–	0.14	0.02
CaO	55.18	54.90	53.79	55.60	54.40	54.81
Na_2O		–	–	–	0.17	0.05
K_2O		–	–	–	0.01	0.02
P_2O_5			trace	trace	0.01	0.07
CO_2	10.83	10.83†	10.83†	10.83†	10.32	10.22
SO_3		0.26	–	–		
F		–	–	–	0.32	0.43
Cl		–	–	–		
H_2O^+	4.43	4.43†	4.43†	4.43†	4.45	4.26
H_2O^-					0.23	0.39
Sum	100.00	99.37	99.55	100.86	99.66	99.48

Notes: empty cells = not determined; dash = less than the accuracy; 1 = analyst V.G. Gmyra (JXA-5a, Central Chem. Lab., Ekaterinburg); 2 and 3 = analyst N.V. Trubkin (JSM+Link ISIS, IGEM, Moscow).
* Henmi et al. (1977).
† Calculated from the ideal composition.

The chemical compositions of both fukalite varieties from Russia are in good agreement with that of the holotype (Table 1). "Monoclinic" fukalite contains even fewer impurities than its orthorhombic analogue. Both fukalite varieties react rapidly with dilute hydrochloric acid, evolving CO_2 bubbles, whereas silica remains in the precipitate.

Infrared spectroscopy

A sample of fukalite preliminarily tested through X-ray powder-diffraction was mixed with anhydrous KBr, pelletized, and analyzed using a two-beam Specord 75 IR spectrophotometer. The IR spectrum of a pure KBr-disk was subtracted from the overall spectrum. Polystyrene and gaseous NH_3 were used as frequency standards; the precision of frequency measurement is ±1 cm^{-1}; the mean resolution for the frequency range 400–1600 cm^{-1} is 0.8 cm^{-1}.

IR spectrum of fukalite (Figs. 1a and 1b) contains characteristic bands of O-H stretching vibrations (in the range 3300–3600 cm^{-1}), carbonate anions (the range 1400–1550 cm^{-1} and narrow bands at 1037 and 860 cm^{-1}), Si-O stretching (the range 887–1140 cm^{-1}) and bending (below 600 cm^{-1}) vibrations. The absence of absorption bands in the range 1550–1700 cm^{-1} indicates the absence of H_2O molecules in fukalite.

The bands with maxima at 3572 and 3587 cm^{-1} correspond to stretching vibrations of OH^- anions coordinating Ca and forming very weak hydrogen bonds. Both bands have non-Voigt shapes (i.e., cannot be described as a convolution of the Gaussian and Lorentzian functions). It means that actually these bands are due to the superposition of absorption bands from different (but similar by their force characteristics) OH groups. The origin of the weak bands at 3395 and 3447 cm^{-1} is unclear.

The CO_3^{2-} groups are strongly polarized. This follows from a very strong splitting of the band of degenerate C-O stretching vibrations (the doublet with band maxima at 1404–1420 and 1523 cm^{-1}, each band being split into several components), as well as from the presence in the IR spectrum of a non-degenerate band of stretching vibrations of CO_3^{2-} groups at 1037 cm^{-1}. The fine structure of the spectrum in the range 1400–1550 cm^{-1} is an indication of local non-equivalence of carbonate groups.

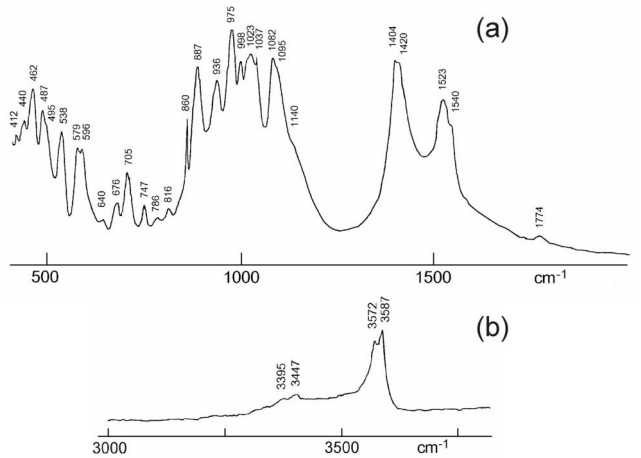

FIGURE 1. IR spectrum of fukalite from the Gumeshevsk deposit.

Vibrations of the batisite-type chain Si_4O_{12} are seen in the IR spectrum of fukalite as a series of well-resolved bands in the ranges of Si-O stretching vibrations (880–1140 cm^{-1}), Si-O-Si bending vibrations (412–538 cm^{-1}), as well as a band of mixed vibrations at 705 cm^{-1}. The IR characteristics of the same vibrations in batisite are as follows: 880–1160, 407–525, and 708 cm^{-1}. In the series of minerals fukalite, batisite, and balangeroite, whose structures contain "*Viereinfachketten*," a regular shift of the position of a main band of Si-O stretching vibrations is observed (975, the doublet 950–973, and 948 cm^{-1}, respectively).

X-ray diffraction data

A structural study of fukalite from Gumeshvesk has been carried out by Rastvetaeva et al. (2005), who found an orthorhombic cell, with a = 3.786, b = 10.916, and c = 23.379 Å, space group $P2_12_12_1$. Rastvetaeva et al. (2005) observed a doubling of the a parameter given by Henmi et al. (1977) and assumed a reference frame with exchanged **a** and **b** vectors with respect to the choice of the Japanese authors. Their structural study, which is the firm starting basis of the present work, has clarified the arrangement of the framework of calcium polyhedra (Fig. 2), which may be described as built up by infinite layers of sevenfold-coordinated calcium polyhedra closely similar to the layers that characterize the structures of all the minerals in the tobermorite group (Merlino et al. 1999, 2000, 2001; Bonaccorsi et al. 2005), and by tilleyite-type layers, built up by zigzag rows of 2 × 1 ribbons of calcium "octahedra." The two layers are connected by corner sharing, and the resulting framework is strengthened through the additional connection afforded by carbonate groups.

The chemical composition and the results of the structural analysis by Rastvetaeva et al. (2005) point to the presence of four-repeat tetrahedral chains (Si_4O_{12}). Both types of calcium-polyhedron layers present a repeat period of 3.8 Å, corresponding to one half of the repeat period of the chains, a situation quite common in various C-S-H (calcium silicate hydrate) compounds, although with a different type of tetrahedral chain.

The framework of Figure 2 presents channels of "pentagonal" shape, running parallel to **a**. The tetrahedral chains Si_4O_{12} may be placed just in those channels, in one of two distinct positions differing by ½ of the repeat period of the chains (~7.6 Å). Due to the disorder in the distribution of the tetrahedral chains, Rastvetaeva et al. (2005) actually refined an "average" structure, presenting a unit translation along **a** of 3.786 Å.

In Figure 3, a structural model including the four-repeat tetrahedral chains is represented as seen along **a**. Due to the geometrical features of the calcium polyhedral framework, we may observe that ambiguities in the positional relationships of the tetrahedral chain may arise in two distinct places, as described by Figure 4. The silicate chains on both sides of the tilleyite ribbons (0-1 and 0-3 in Fig. 3) have x coordinates that differ by ±¼ (in terms of the chain period, which is 7.572 Å). Similarly, chains located on opposite sides of the tobermorite-like layer of calcium polyhedra (0-2 in Fig. 3) have x coordinates that differ by ±¼.

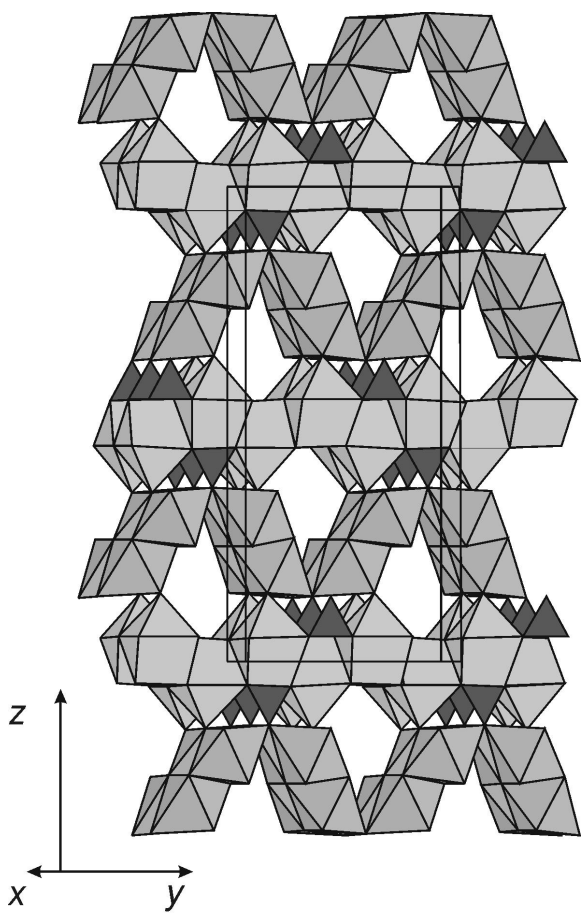

FIGURE 2. The calcium-polyhedron scaffolding as seen down **a**, with a small tilt (10°) to give a better view of the structural arrangement (data from Rastvetaeva et al. 2005).

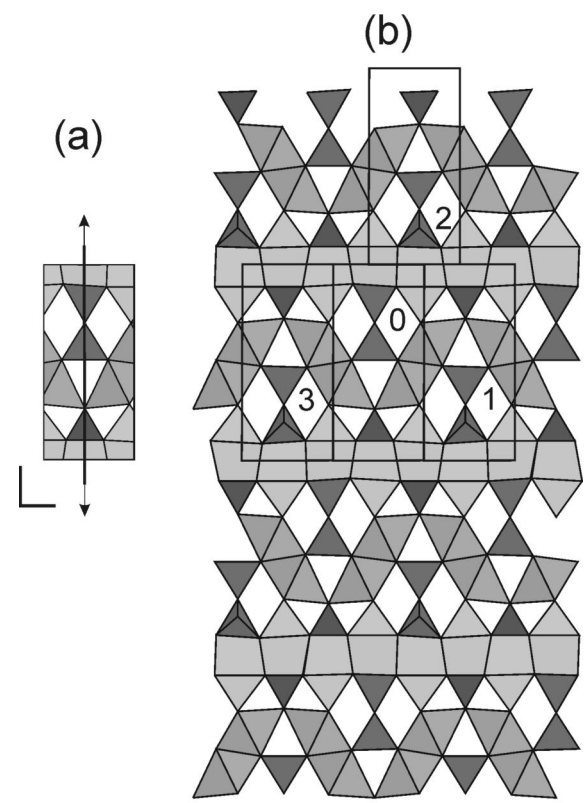

FIGURE 3. (**a**) Schematic drawing of the rod, with the indication of the symmetry operators; (**b**) structural model including the four-repeat tetrahedral chains, represented as seen along **a**, with **b** horizontal.

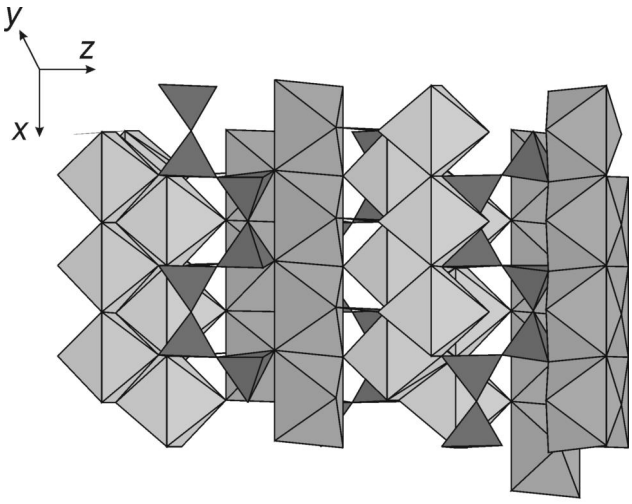

FIGURE 4. Structural model as seen normal to (010) [with a small tilt of 5°], **a** vertical, **c** horizontal, to appreciate the connection of the silicate chains with the two types of calcium polyhedral layers.

Fukalite as an OD structure built up with equivalent rods

The structure presents the character of an order-disorder (OD) structure built up with rods of one type, distributed according to a scheme of two-dimensional disorder. A clever and insightful use of structural rods, together with the concepts of OD theory, has been made by Belokoneva (2005) and Belokoneva et al. (1998), in describing and discussing the crystal chemical relationships in broad borate families. However, there are few examples of OD structures built up by rods with ambiguity of rod stacking in two directions, only one fully analyzed by Dornberger-Schiff (1964a). No systematic theory for this kind of OD structures exists, in contrast to the case of OD structures built up with equivalent layers and one-dimensional disorder. However, it is possible to apply to this class of OD structures the concepts and the procedures already developed for the more frequently occurring OD structures with one-dimensional disorder.

As in the case of OD layers, also in the case of the structures built with OD rods, it will be necessary to indicate the partial operations (PO) of λ type (which bring a rod into itself) and of σ type (which bring a rod into the adjacent ones). In Figure 3, a rod, denoted 0, is indicated; it has dimensions a_0 7.572, b_0 5.458 (=10.916/2), and c_0 11.690 (=23.379/2) Å, rod symmetry *Pmm*2. Similarly to the case of one-dimensional disorder, in which the group of λ symmetry operations corresponds to one of the 80 layer groups, in the case of the OD structures built up by rods the group of λ symmetry operations corresponds to one of the 75 groups of rods (Kopský and Litvin 2006). Besides the rod 0, other rods (1, 2, 3) are indicated. On the basis of the previous statement [coordinates x different by ±¼ in adjacent rods placed on opposite sides of octahedral ribbons (for example 0-1) and of calcium polyhedra (for example 0-2)], assuming a coordinate $x = 0$ for the rod 0, rods 1, 2, 3 will have coordinates $x = \pm 1/4$. A schematic representation of the distribution of the rods with symmetry *Pmm*2 (projection in the **b**,**c** plane) is given in Figure 5; in it the single rods are represented by isosceles triangles that reflect the *mm*2 symmetry. Besides rod 0, the rods 1, 2 (and 2′), 3, 4, 5, 6, 7, 8 (and 8′), and 9 are indicated. The rods 1, 2 (and 2′), 3, and 4 have coordinate $x = \pm 1/4$, the rods 5, 6, 7, 8 (and 8′), and 9 have coordinates x of 0 or ½. In the schematic representation, the white triangles correspond to rods located at 0, ½ (along **a**); the dark gray triangles correspond to rods located at ±¼.

An OD structure of rods occurs when the following condition is satisfied: pairs of adjacent rods that present equivalent projections are geometrically equivalent everywhere in the structure. For example, the pairs 0-1 and 2-9 are geometrically equivalent. This definition requires that the adjacency of a given rod has to be clearly indicated. To this aim, it will be sufficient to indicate the rods that are adjacent to rod 0 (adjacency of rod 0); from the OD character of the structure the adjacency of any other rod will follow. The adjacency of the rod 0 (white triangle) is given by the rods 1, 2 (and 2′), 3 (obviously indicated by gray triangles).

As in the case of the one-dimensional disorder, the symbol that describes the symmetry properties common to the whole family of OD structures has to present the set of operations that transform a rod into itself (λ-POs, i.e., partial operations λ) and the various sets of operations that transform the rod 0 into the adjacent rods (σ-POs).

$$\begin{array}{llll} P & m & (m) & (2) \\ & \{2_{1/2} & (2_2) & (n_{1/2,2})\} \quad 0-1; \quad 0-3 \\ & \{2_{1/2} & (2_1) & (n_{1/2,1})\} \quad 0-2; \quad 0-2' \end{array} \tag{1}$$

The notations for the σ-POs closely correspond to those introduced by Dornberger-Schiff in her theory of OD structures built up with equivalent layers (Dornberger-Schiff 1956, 1964b, 1966; Ďurovič 1997; Merlino 1997; Ferraris et al. 2008), and follow the system of the international notations for space group operations. For example, $2_{1/2}$ in the first position of the second

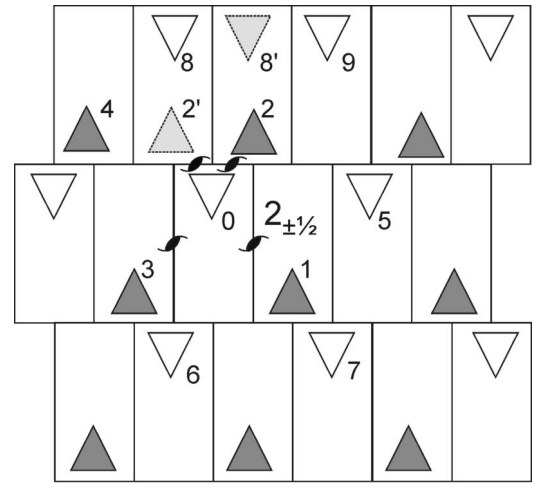

FIGURE 5. Schematic representation of the distribution of the rods (represented by isosceles triangles that reflect the *mm*2 symmetry) in the crystal structure of fukalite. The white triangles correspond to rods located at 0, ½ (along **a**); the dark gray triangles correspond to rods located at ±¼. The light dashed gray triangles 2′ and 8′ represent alternative positions for 2 and 8 rods, respectively. The twofold screw axes are $2_{\pm 1/2}$.

TABLE 2. Unit-cell parameters (in Å and degrees) calculated on the basis of the data presented by Rastvetaeva et al. (2005) and space groups for MDO structures in fukalite family

	a	*b*	*c*	α	β	γ	Space group	Matrix
MDO1	7.572	11.554	23.379			109.13	$P112_1/b$	$200/\bar{1}10/001$
MDO2	7.572	11.554	12.004	77.6	90.0	109.13	$P\bar{1}$	$200/1\bar{1}0/0¼½$
MDO3	7.572	10.916	23.379		90.0		$P12_1/c1$	200/010/001
MDO4	7.572	10.916	12.004	103.14	90.0	90.0	$P\bar{1}$	$200/010/0\bar{1}¼½$
MDO5	7.572	10.916	23.685		99.2		$P12_1 1$	$200/010/\bar{1}01$
MDO6	7.572	10.916	24.009	103.14	90.0	90.0	$B\bar{1}$	$200/010/0\bar{1}½1$

Note: In the last column, the transformation matrix to pass from the unit cell given by Rastvetaeva et al. (2005) to the cell of the various MDO structures is shown.

row of the symbol 1 indicates a twofold screw axis parallel to **a** with translation component **a**/4; 2_2 in the second position indicates a twofold axis parallel to $\mathbf{b}_0$, with translation component $\mathbf{b}_0$; $n_{1/2,2}$ in the third position indicates a *n* glide normal to $\mathbf{c}_0$ with translation component $\mathbf{a}/4 + \mathbf{b}_0$. As in the case of the OD structures built up by equivalent layers, the parentheses indicate the directions of missing periodicities.

As indicated by the symbol, the set of σ-POs relating the rods 0 and 1, is valid also for the pair 0-3. The other set of σ-POs indicates that rod 2 is located, with respect to rod 0 assumed at 0, 0, *z*, at ¼, ½, –*z*, through the application of the operation [– – $n_{1/2,1}$]; actually due to the *mm*2 symmetry of rod 0, the whole set of operations [– – $n_{\pm1/2,\pm1}$] gives rise to geometrically equivalent pairs of rods, with rods located at ¼, ½, –*z* and –¼, ½, –*z* (rods 2), and also at ¼, –½, –*z*, and –¼, –½, –*z* (rods 2′). Obviously the position 2 and 2′ are mutually exclusive and their occurrence is correlated with the occurrence of 8 and 8′, respectively.

Also in the case of rod 2 there are four possible positions for the adjacent rod 0, namely 0, 0, *z* and ½, 0, *z* and also 0, 1, *z* and ½, 1, *z*. By applying the same considerations to the various rods, an average structure (family structure in OD terminology) is obtained; it displays space group symmetry *Amma*, with *a* = 3.786, *b* = 5.458, *c* = 23.379 Å, in keeping with the results presented by Henmi et al. (1977), who, by assuming a reference frame with interchanged **a** and **b** vectors, indicate $Bm2_1b$, *Bmmb*, and *B*2*mb* as possible space groups for the family structure.

MDO Structures

An infinite number of disordered and ordered (polytypes) arrangements of rods exist, corresponding to the σ operations indicated above. As in the case of OD structures with one-dimensional disorder, a limited number of ordered structures display maximum degree of order (MDO). In the case of the one-dimensionally disordered structures, MDO structures are those in which triples of subsequent layers are equivalent, everywhere taken in the structure. This definition has been properly extended by Dornberger-Schiff (1964a) to deal with OD structures built up with rods. Whereas in the Appendix[1] we shall present that extended definition and suggest a procedure to derive MDO structures in the fukalite family, we report here (Table 2) the results obtained.

STRUCTURE SOLUTION AND REFINEMENT

Several crystals of fukalite were selected from the Gumeshevsk deposit sample and mounted on the X-ray diffraction beamline XRD1, at the Elettra synchrotron facility (Basovizza-Trieste, Italy). After several trials a crystal was found that showed a good degree of structural order, indicated by relatively strong and sharp polytypic reflections. The wavelength of the radiation was set to 1.0 Å, and the crystal was placed at the distance of 36 mm from a 165 mm MarCCD detector.

TABLE 3. Crystal data and structure refinement for fukalite from Gumeshevsk, polytype MDO1

Empirical formula	$Ca_8Si_4O_{12}(OH)_4(CO_3)_2$	
Formula weight	813.05	
Wavelength	1.0 Å	
Crystal system	Monoclinic	
Space group	$P2_1/c$	
Unit-cell dimensions	*a* = 7.573(3) Å	
	b = 23.364(5) Å	β = 109.15(1)°
	c = 11.544(4) Å	
Volume	1929.5(11) Å^3	
Z	4	
Density (calculated)	2.799 g/cm^3	
Crystal size	0.15 × 0.10 × 0.05 mm^3	
Theta range for data collection	2.45 to 30.01°	
Index ranges	$-7 \le h \le 7$, $-23 \le k \le 21$, $-11 \le l \le 11$	
Reflections collected	7004	
Independent reflections	1958 [*R*(int) = 0.0214]	
Absorption correction	Semi-empirical from equivalents	
Refinement method	Full-matrix least-squares on F^2	
Data / restraints / parameters	1958 / 0 / 206	
Goodness-of-fit on F^2	1.111	
Final *R* indices [$I > 2\sigma(I)$]	*R*1 = 0.0342, *wR*2 = 0.1005	
R indices (all data)	*R*1 = 0.0352, *wR*2 = 0.1022	
Largest diff. peak and hole	0.452 and –0.560 e·Å^{-3}	

The crystal was rotated around the φ axis by steps of 3°, and 7004 reflections were recorded and processed with the HKL package of programs (XDISP, DENZO, and SCALEPACK, Otwinowski and Minor 1997). The data were finally corrected for absorption effects with the program MULABS in WinGX (Farrugia 1999) on the basis of the intensities of equivalent reflections. The refined monoclinic unit-cell parameters were *a* = 7.573 (3), *b* = 23.364 (5), *c* = 11.544 (4) Å, and β = 109.15(1)°, corresponding to the MDO1 polytype. A standard orientation of the unit cell was chosen, different from the orientation assumed in Table 2; this orientation will be used in the description and discussion of the structural arrangement. Additional information on the data collection and structure refinement can be found in Table 3.

The starting atomic coordinates were obtained on the basis of

[1] Deposit item AM-09-011, Tables 9–13, Appendix MDO Structures in the fukalite family, Appendix Table 1, Appendix Figure 1, and a CIF data set. Deposit items are available two ways: For a paper copy contact the Business Office of the Mineralogical Society of America (see inside front cover of recent issue) for price information. For an electronic copy visit the MSA web site at http://www.minsocam.org, go to the American Mineralogist Contents, find the table of contents for the specific volume/issue wanted, and then click on the deposit link there.

the structural model obtained through the OD theory (described in the preceding paragraphs), as regards both the calcium polyhedral layers and the ordered position of the silicate chains. The carbonate groups were localized after Fourier synthesis. The refinement was performed by using the program SHELXL (Sheldrick 1997). It proceeded smoothly and, after introducing anisotropic displacement parameters for the calcium and silicon cations, converged to $R = 0.037$ for 1958 independent reflections. In the final difference Fourier map, the highest electron density maxima were found to correspond to the positions of hydrogen atoms belonging to four hydroxyl groups. Those maxima were introduced in the atomic list, but their positions were not refined. The final least-squares refinement cycles resulted in a reliability index R of 0.0342 for 1848 reflections with $I > 2\sigma(I)$ and 0.0352 for all 1958 data.

The final positional and displacement parameters are reported in Tables 4 and 5, respectively. Bond distances are given in Table 6. The list of the F_o-F_c values and a CIF file of the refinement are available as supplemental material.[1]

Description of the crystal structure of fukalite

The crystal structure of fukalite from Gumeshevsk, Central Urals, Russia (MDO1 polytype) is reported in Figure 6. The calcium polyhedral framework largely corresponds to the description given by Rastvetaeva et al. (2005), apart from minor details and a higher precision in bond distances. It is built by two distinct modules, which are described in the following.

Tobermorite-like layer of seven-coordinated calcium polyhedra. The coordination of calcium in the tobermorite-like layer has been already described by Hoffmann and Armbruster

TABLE 4. Atomic coordinates and equivalent isotropic displacement parameters (Å²) for fukalite from Gumeshevsk, polytype MDO1

	x	y	z	U_{eq}
Ca1	0.4339(1)	0.0436(1)	0.1247(1)	0.012(1)
Ca1A	0.9391(1)	0.0437(1)	0.1237(1)	0.012(1)
Ca4	0.3111(1)	−0.0452(1)	0.3734(1)	0.012(1)
Ca4A	0.8112(1)	−0.0457(1)	0.3737(1)	0.013(1)
Ca2	0.2768(2)	−0.3094(1)	0.3037(1)	0.015(1)
Ca2A	0.7776(2)	−0.3091(1)	0.3074(1)	0.014(1)
Ca3	0.5957(2)	−0.1932(1)	0.4398(1)	0.014(1)
Ca3A	0.0963(2)	−0.1929(1)	0.4435(1)	0.014(1)
Si1	0.4743(2)	−0.0860(1)	0.1237(1)	0.014(1)
Si1A	0.8998(2)	−0.0863(1)	0.1257(1)	0.014(1)
Si2	0.3946(2)	−0.2179(1)	0.1218(1)	0.015(1)
Si2A	0.9798(2)	−0.2182(1)	0.1274(1)	0.015(1)
C1	0.3117(6)	0.0816(2)	0.3764(3)	0.010(1)
C1A	0.8149(6)	0.0796(2)	0.3761(3)	0.011(1)
O1	0.1192(5)	0.0506(1)	−0.0049(3)	0.014(1)
O1A	0.6267(5)	0.0489(1)	−0.0037(3)	0.013(1)
O2	0.4915(5)	−0.0480(1)	0.2429(2)	0.013(1)
O2A	0.0014(5)	−0.0473(1)	0.2436(2)	0.013(1)
O3	0.3657(6)	0.0515(1)	0.4774(3)	0.016(1)
O3A	0.8632(6)	0.0496(1)	0.4773(3)	0.016(1)
O4	0.2616(6)	0.0538(1)	0.2740(3)	0.017(1)
O4A	0.7608(6)	0.0518(1)	0.2735(3)	0.016(1)
O5	0.3164(4)	0.1353(1)	0.3792(2)	0.020(1)
O5A	0.8143(4)	0.1332(1)	0.3786(2)	0.021(1)
O6	0.5335(4)	−0.2421(1)	0.2457(2)	0.019(1)
O6A	−0.0246(4)	−0.2432(1)	0.2542(2)	0.019(1)
O7	0.3967(4)	−0.2413(1)	−0.0067(2)	0.019(1)
O7A	0.8411(4)	−0.2409(1)	0.0017(2)	0.019(1)
O8	0.1865(4)	−0.2414(1)	0.1246(2)	0.019(1)
O8A	0.6880(4)	−0.1011(1)	0.1275(2)	0.021(1)
O9	0.3808(4)	−0.1479(1)	0.1236(2)	0.020(1)
O9A	0.9952(4)	−0.1482(1)	0.1311(3)	0.020(1)
OH1	0.3091(4)	−0.1443(1)	0.3736(2)	0.013(1)
OH1A	0.8174(4)	−0.1437(1)	0.3784(2)	0.013(1)
OH2	0.4434(4)	0.1423(1)	0.1298(2)	0.013(1)
OH2A	0.9347(4)	0.1434(1)	0.1242(2)	0.014(1)
H1	0.2763	−0.1503	0.2997	0.050
H1A	0.7735	−0.1509	0.2973	0.050
H2	0.3970	0.1509	0.0516	0.050
H2A	0.8984	0.1479	0.0450	0.050

Notes: U_{eq} is defined as one third of the trace of the orthogonalized U_{ij} tensor.

TABLE 5. Anisotropic displacement parameters (Å² x 10³) for fukalite from Gumeshevsk, polytype MDO1

	U_{11}	U_{22}	U_{33}	U_{23}	U_{13}	U_{12}
Ca1	0.009(1)	0.014(1)	0.012(1)	0.000(1)	0.002(1)	0.000(1)
Ca1A	0.008(1)	0.014(1)	0.011(1)	0.000(1)	0.002(1)	0.000(1)
Ca4	0.009(1)	0.015(1)	0.011(1)	0.000(1)	0.002(1)	0.000(1)
Ca4A	0.010(1)	0.015(1)	0.013(1)	0.001(1)	0.003(1)	0.000(1)
Ca2	0.012(1)	0.016(1)	0.013(1)	−0.001(1)	0.000(1)	0.001(1)
Ca2A	0.011(1)	0.015(1)	0.013(1)	0.000(1)	0.001(1)	0.000(1)
Ca3	0.011(1)	0.014(1)	0.013(1)	−0.001(1)	0.000(1)	0.000(1)
Ca3A	0.013(1)	0.016(1)	0.012(1)	−0.001(1)	0.001(1)	0.000(1)
Si1	0.014(1)	0.015(1)	0.013(1)	0.000(1)	0.002(1)	0.000(1)
Si1A	0.014(1)	0.014(1)	0.013(1)	0.000(1)	0.002(1)	0.001(1)
Si2	0.016(1)	0.016(1)	0.012(1)	0.000(1)	0.002(1)	0.001(1)
Si2A	0.016(1)	0.016(1)	0.012(1)	0.000(1)	0.002(1)	0.000(1)

Notes: The anisotropic displacement factor exponent takes the form: $-2\pi^2[h^2a^{*2}U_{11} + ... + 2hka^*b^*U_{12}]$.

TABLE 6. Selected bond distances (Å) in fukalite from Gumeshevsk, polytype MDO1

Ca1-OH2	2.308(3)	Ca1A-O1	2.327(4)
-O1	2.367(4)	-OH2A	2.330(3)
-O1A	2.400(4)	-O1A	2.344(4)
-O4	2.492(4)	-O2A	2.496(3)
-O2	2.498(3)	-O4	2.501(4)
-O4A	2.515(4)	-O4A	2.526(4)
-O1A	2.531(3)	-O1	2.556(3)
Average	**2.444**	**Average**	**2.440**
Ca2-OH2	2.299(3)	Ca2A-OH2	2.326(3)
-OH2A	2.312(3)	-OH2A	2.340(3)
-O7	2.390(3)	-O6	2.347(3)
-O5A	2.397(3)	-O6A	2.365(3)
-O8	2.518(3)	-O5	2.415(3)
-O6A	2.659(3)	-O7A	2.431(3)
-O6	2.748(3)	**Average**	**2.371**
Average	**2.475**		
Ca3-OH1A	2.332(3)	Ca3A-OH1A	2.304(3)
-O7A	2.338(3)	-OH1	2.322(3)
-OH1	2.348(3)	-O6A	2.383(3)
-O7	2.368(3)	-O5A	2.389(3)
-O5	2.393(3)	-O8	2.501(3)
-O6	2.420(3)	-O7	2.648(3)
Average	**2.367**	-O7A	2.726(3)
		Average	**2.468**
Ca4-OH1	2.317(3)	Ca4A-OH1A	2.289(3)
-O2A	2.333(4)	-O2	2.397(4)
-O2	2.343(4)	-O2A	2.398(4)
-O3A	2.493(4)	-O3A	2.498(3)
-O3	2.492(4)	-O3A	2.503(4)
-O3	2.526(3)	-O3	2.505(4)
-O4	2.554(3)	-O4A	2.527(3)
Average	**2.437**	**Average**	**2.445**
Si1-O1A	1.601(3)	Si1A-O1	1.592(3)
-O2	1.607(3)	-O9A	1.608(3)
-O9	1.608(3)	-O2A	1.610(3)
-O8A	1.643(3)	-O8A	1.647(3)
Average	**1.615**	**Average**	**1.614**
Si2-O6	1.577(3)	Si2A-O7A	1.578(3)
-O7	1.586(3)	-O6A	1.586(3)
-O9	1.641(3)	-O9A	1.639(3)
-O8	1.678(3)	-O8	1.666(3)
Average	**1.621**	**Average**	**1.617**
C1-O5	1.256(6)	C1A-O5A	1.252(6)
-O4	1.291(5)	-O4A	1.295(5)
-O3	1.307(5)	-O3A	1.307(5)
Average	**1.285**	**Average**	**1.285**

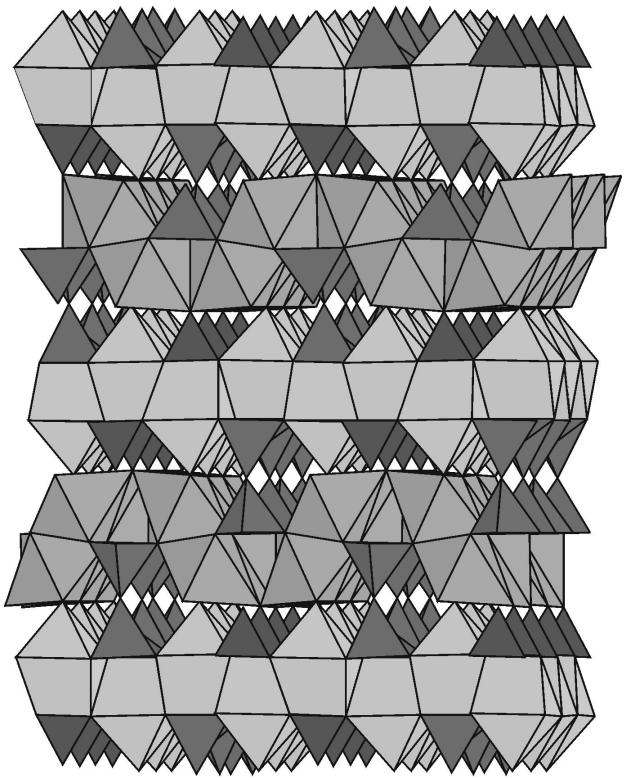

FIGURE 6. Crystal structure of fukalite from Gumeshevsk, MDO1 polytype, as seen down [1 0 0], **b** vertical, with a slight tilt (–10°) to give a better view of the structural arrangement.

(1997) and Merlino et al. (2000) in their papers on the family structure and real structure of clinotobermorite, respectively, as consisting of "a pyramidal part on one side and a dome part on the other side joining the equatorial oxygen atoms" (Fig. 7). There are four crystallographically independent polyhedra in the layer, centered by Ca1, Ca1A, Ca4, and Ca4A. In the polyhedra centered by Ca4 and Ca4A (Fig. 8a), the calcium cations lie in the center of the basal plane of the pyramid, whereas in those centered by Ca1 and Ca1A the calcium cations are slightly displaced from the basal plane of the pyramid toward the domatic part (Fig. 8b).

The data presented in Figures 8a and 8b indicate that the dome edge of the Ca1 and Ca1A polyhedra is substantially shorter than the two edges of the pyramidal bases parallel to it (~2.61 Å, to compare with ~3.00–3.03 Å), a geometrical feature that is related to the connection between the tobermorite-like like calcium layer and the silicate chain (Fig. 7), as will be discussed later on. The dome edge of the Ca4 and Ca4A polyhedra is even shorter (~2.22 Å), as it corresponds to the shared edge of the carbonate group.

Ca1 and Ca1A polyhedra, as well as Ca4 and Ca4A polyhedra, alternate along **a,** forming columns of edge-sharing polyhedra presenting coplanar pyramidal bases. These columns adjoin each other, once more through edge sharing, along **c**, in such a way that adjacent columns present the pyramidal apical ligands on opposite sides of the resulting infinite layers parallel to (010). Those apical ligands are hydroxyl anions, located at the common corner between the tobermorite-type and the tilleyite-type layers.

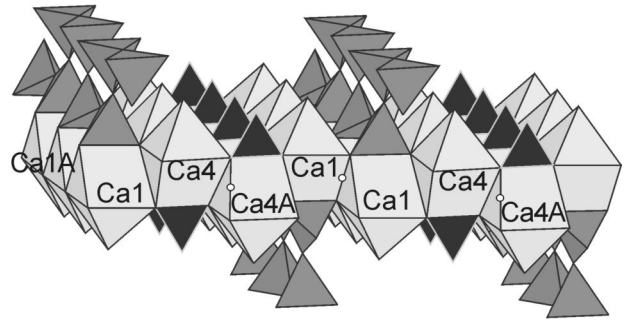

FIGURE 7. Tobermorite-type layer of seven-coordinated calcium polyhedra (light gray) with silicate chains (dark gray) and carbonate groups (black) linked on both sides. Small circles indicate inversion centers.

Tilleyite-type layer of seven-coordinated and six-coordinated calcium polyhedra. The arrangement of calcium polyhedra in the tilleyite-type layer closely corresponds to that occurring in the tilleyite bands, introduced by Belov (1963) as constituting modules in various C-S-H compounds. The tilleyite band in fukalite is illustrated in Figure 9, where not only the corrugated wall of calcium polyhedra, but also the silicate chains and rows of carbonate groups linked to the wall are represented. It seems useful to remark that, whereas the "ideal" tilleyite bands are built up with columns of calcium octahedra, the actual tilleyite bands in several calcium silicate compounds, including tilleyite itself (Louisnathan and Smith 1970; Grice 2005) present coordination polyhedra with six, seven, and even eight ligands. In fukalite columns of edge-sharing alternating sixfold (Ca2A, Ca3) and sevenfold (Ca2, Ca3A) coordinated calcium polyhedra run along **a** and are connected by edge-sharing to build 2 × 1 ribbons. Each ribbon is linked to adjacent ribbons to build up the corrugated walls parallel to (010).

Also in this case there are four crystallographically independent polyhedra, centered by Ca2, Ca3, Ca2A, and Ca3A, in each wall. The polyhedra centered by Ca2A and Ca3 (Fig. 10a) are substantially regular octahedra with an average bond distance of 2.364 Å, whereas those centered by Ca2 and Ca3A are highly distorted mono-capped octahedra, presenting bond distances closely similar to each other, with values distributed as indicated in Figure 10b. The three longest distances are those involving O8 (the shared O atom between Si2 and Si2A tetrahedra), with bond distances Ca2-O8 2.518 Å, Ca3A-O8 2.501 Å, and those involving O6, O6A and O7, O7A, namely the pairs of O atoms aligned along **a** in the Si2-Si2A "paired" tetrahedra (Ca2-O6 2.748 Å, Ca2-O6A 2.659 Å, and Ca3A-O7 2.648 Å, Ca3A-O7A 2.726 Å).

Silicate chains Si_4O_{12}. Infinite silicate chains with repeat every fifth tetrahedron ["*Viererketten*" in the classification of Liebau (1956, 1985)] run along **a** and are linked to the tobermorite-type and to the tilleyite-type layers on opposite sides. "*Viererreinfachketten*" of such composition have been already found in several natural and synthetic compounds. Table 7 lists those that present a conformation closely similar to that of fukalite, although characterized by different periodicities: from the strongly folded chain in haradaite (Takéuchi and Joswig 1967; Basso et al. 1995) to the very extended chain in balangeroite (Ferraris et

al. 1987). The folding is obtained by decreasing the Si···Si···Si angles, as clearly shown by the data presented in Table 7, and allows a stable connection of the chains to the other polyhedral modules that characterize the various structural arrangements. In haradaite and in $BaUO_2Si_2O_6$, the loops between the chain tetrahedra are closed by VO_5 and UO_6 groups, respectively. In ohmilite and batisite, the chains are linked to infinite chains of corner-sharing TiO_6 octahedra. In balangeroite, the tetrahedral chains are linked to 3×1 ribbons of edge-sharing Mg octahedra. The extension of the silicate chains is required to span the unit period of 9.6 Å, corresponding to three times the length of an octahedral edge (see Fig. 4 in Ferraris et al. 1987). In fukalite, the chains are folded just in such a way that the repeat period along the chain is consistent with the period of the columns of calcium polyhedra.

TABLE 7. Repeat period and Si···Si···Si angles for *"Viereinfachketten"* with different degree of folding

Phase	Period (Å)	Angle (°)	Reference
Haradaite	7.031	96.1	Takéuchi and Joswig 1967; Basso et al. 1995
$BaUO_2Si_2O_6$	7.496	101.1	Plaisier et al. 1995
Fukalite	7.573	101.0	this paper
Ohmilite	7.799	104.1	Mizota et al. 1983
Batisite	8.140	106.6	Rastvetaeva et al. 1997
Balengeroite-2*M*	9.60	126.6	Ferraris et al. 1987

The chains may be described as built through the connection of two distinct pairs of disilicate groups, Si1-Si1A and Si2-Si2A, and are firmly linked to the tilleyite-like layer through the Si2-Si2A "paired" tetrahedra, each sharing two edges with Ca2 and Ca3A polyhedra, with distances from 2.523 to 2.540 Å, as well as to the calcium tobermorite-like layer through the Si1-Si1A "paired" tetrahedra, which share the "dome" edges of the Ca1, Ca1A polyhedral columns (edge lengths of 2.608 and 2.605 Å, respectively). A perfect adjustment is obtained through a flexing of the Si2-Si2A "paired" tetrahedra, which results in lowering the Si2-O8-Si2A angle to 142.0°, to compare with the value for the other "paired" tetrahedra (Si1-O8A-Si1A, 155.4°), as well as with the values 150.0° and 150.3° for Si1-O9-Si2 and Si1A-O9A-Si2A, respectively. Through that flexing, the edges parallel to **c** of the Si1, Si1A tetrahedra succeeding each other along **a**, are at a constant distance of nearly 3.8 Å, thus closely fitting with the dome edges of the Ca1, Ca1A polyhedra.

Rows of carbonate groups. The last module in the structure of fukalite is the row of CO_3 groups parallel to (100) and stacked along **a**. The carbonate groups share the "dome" edges of the

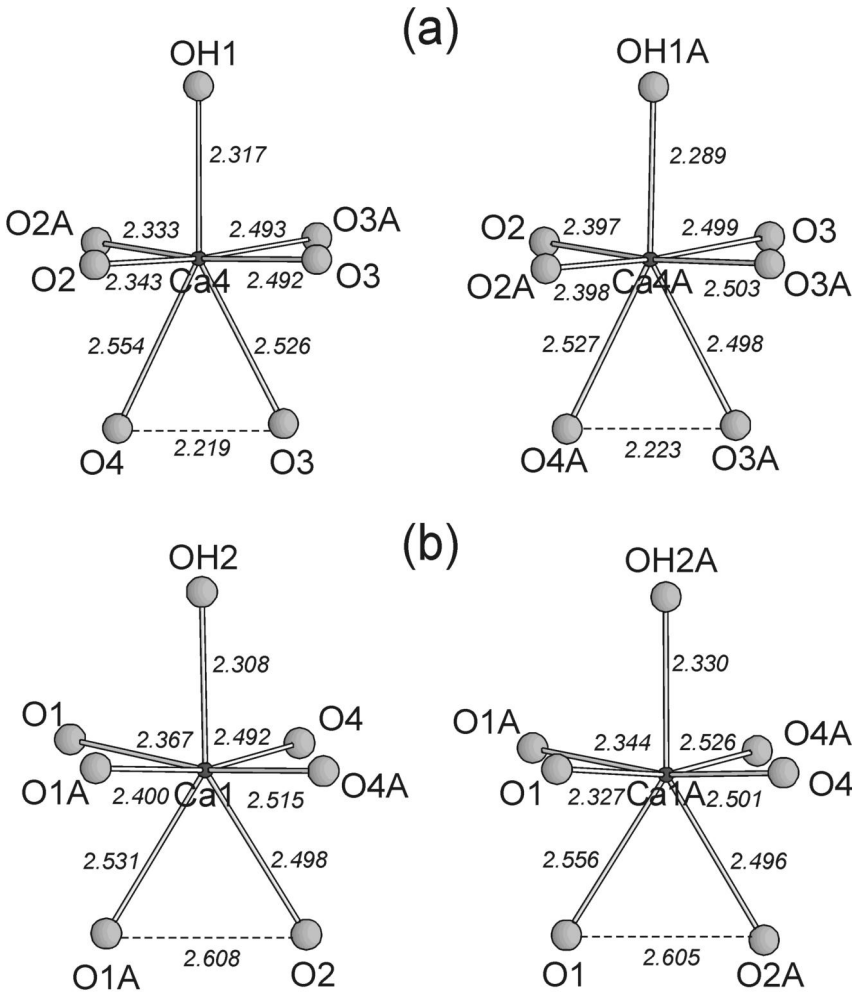

FIGURE 8. Four crystallographically independent polyhedra in the tobermorite-type layer. The Ca-O distances (Å) are shown. The dashed lines indicate O-O distances significantly shorter then the average ones.

Ca4, Ca4A polyhedral columns (edge lengths of 2.219 and 2.223 Å, respectively) on one side, and are corner-linked to the tilleyite-type layer on the other side, at the O5 and O5A sites, respectively. The two independent carbonate groups are planar, with C-O bond distances of 1.30 Å for the oxygen atoms of the shared edges (O-C-O angles of 117°) and 1.26 Å for the corner-shared oxygen atoms (O-C-O angles of 121.5°).

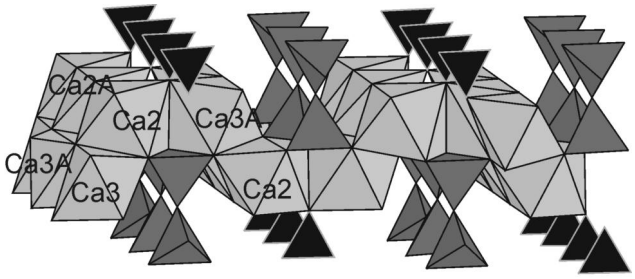

FIGURE 9. Tilleyite-type layer of six- and seven-coordinated calcium polyhedra (light gray) with silicate chains (dark gray) and carbonate groups (black) grasped on both sides.

In the crystal structure of fukalite the two distinct layers of calcium polyhedra are connected through the silicate chains and the carbonate groups, as previously described. Moreover they are also directly connected through the pyramidal apical ligands of the Ca1, Ca1A, Ca4, and Ca4A polyhedra. As stated, those apical ligands are hydroxyl anions, as indicated by the results of the difference Fourier calculations, which showed residual peaks near their positions (corresponding to the hydrogen sites H1, H1A, H2, and H2A), and of the bond-valence balance calculations, which have been performed with the parameters given by Brese and O'Keeffe (1991). The bond-valence sums for the various oxygen atoms are given in Table 8. The low valence sum for the oxygen atom O8A (1.88 v.u.) is balanced by two hydrogen bonds with the hydroxyl groups OH1A (O···O distance 2.911Å) and OH2 (O···O distance 2.967 Å). Very weak and bifurcated hydrogen bonds occur between OH1 and OH2A hydroxyl groups and the oxygen atoms O9 and O9A, as indicated in Figure 11. The last column of Table 8 presents the valence sums for the various anions corrected for the hydrogen bond contribution, calculated from the OH···O bond distance according to the suggestion of Ferraris and Ivaldi (1988).

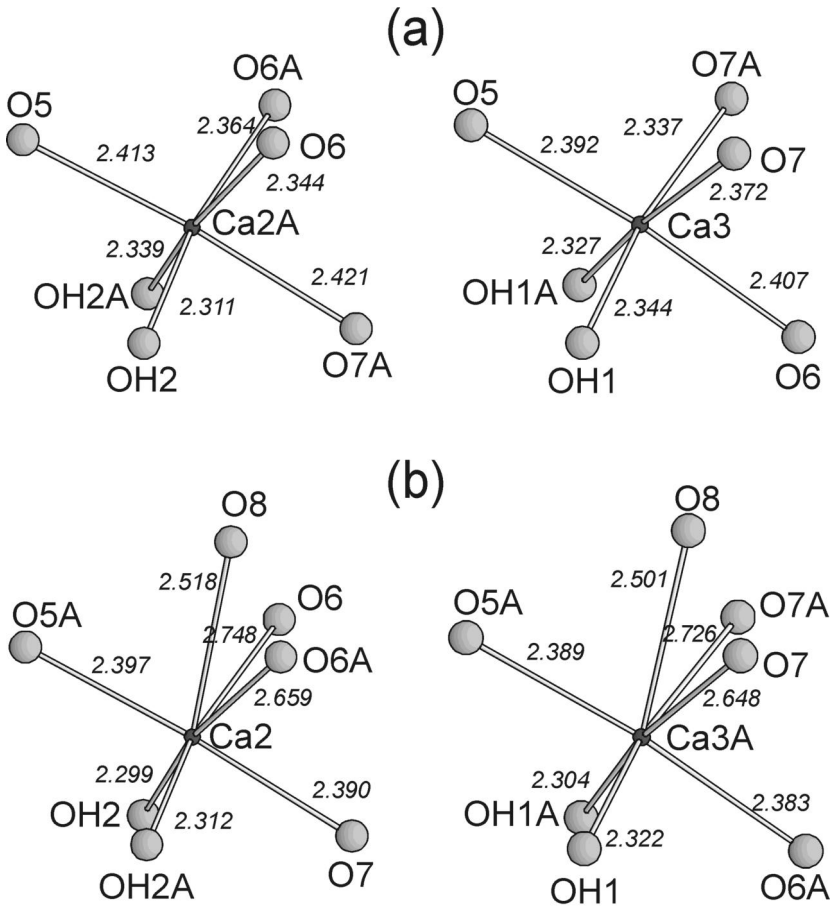

FIGURE 10. Four crystallographically independent polyhedra in the tilleyite-type layer. The Ca-O distances (Å) are reported.

TABLE 8. Valence bond calculation for fukalite from Gumeshevsk, polytype MDO1

	Ca1	Ca1A	Ca2	Ca2A	Ca3	Ca3A	Ca4	Ca4A	Si1	Si1A	Si2	Si2A	C1	C1A	Σ_{anions}	Σ'_{anions}
O1	0.34	0.38								1.09					2.01	
		0.20														
O1A	0.31	0.36							1.06						1.95	
	0.22															
O2	0.24						0.36	0.31	1.05						1.96	
O2A		0.24					0.37	0.31		1.04					1.96	
O3							0.24	0.23					1.25		1.95	
							0.22									
O3A							0.24	0.24						1.25	1.97	
								0.23								
O4	0.24	0.24					0.20						1.31		1.99	
O4A	0.23	0.22						0.22						1.29	1.96	
O5				0.30	0.32								1.44		2.05	
O5A			0.31			0.32								1.45	2.08	
O6			0.12	0.36	0.29						1.14				1.91	
O6A			0.15	0.34		0.32						1.11			1.93	
O7			0.32		0.34	0.16					1.11				1.92	
O7A				0.29	0.37	0.13						1.13			1.91	
O8			0.23			0.24					0.86	0.89			2.22	
O8A									0.95	0.94					1.89	2.18
O9									1.04		0.96				2.00	2.23
O9A										1.04		0.96			2.00	2.24
OH1					0.36	0.38	0.39								1.13	0.89
OH1A					0.37	0.40		0.42							1.19	1.04
OH2	0.40		0.41	0.38											1.18	1.05
OH2A		0.37	0.39	0.36											1.13	0.91
$\Sigma_{cations}$	1.97	2.01	1.93	2.03	2.05	1.95	2.03	1.97	4.11	4.11	4.06	4.09	3.99	4.00		

Notes: The bond strengths (v.u.) were calculated following Brese and O'Keeffe (1991); in the last column the valence sums for the various anions were corrected for the hydrogen bond contributions (Ferraris and Ivaldi 1988).

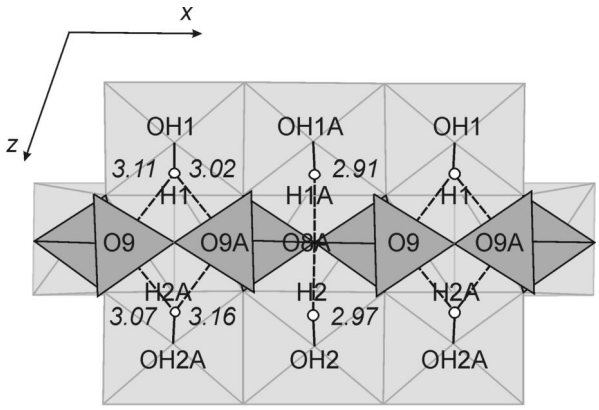

FIGURE 11. Hydrogen-bond scheme in fukalite from Gumeshevsk, MDO1 polytype. The positions of the hydrogen atoms, held fixed during the refinement, are represented by small white circles. The O···O distances (Å) are indicated.

CONCLUDING REMARKS

The results of the present study indicate that other MDO structures could be found from the same or other localities, as well as in specimens of $Ca_4Si_2O_6(CO_3)(OH)_2$ prepared in the laboratory. It is well known that novel sodium lanthanide silicates with the structure-type of tobermorite 11 Å and characterized by the substitution $Na^+ + Ln^{3+} = 2\ Ca^{2+}$ (with Ln indicating one of the lanthanide atoms) have been prepared (Ferreira et al. 2003; Merlino et al. 2008.). The presence of the tobermorite-type module in the structure of fukalite points to the possible preparation of silicates with the structure-type of fukalite and composition $NaLnCa_2Si_2O_6(CO_3)(OH)_2$ where the substitution $Na^+ + Ln^{3+} = 2\ Ca^{2+}$ takes place in the tobermorite-type module, and also of silicates with composition $Na_2Ln_2Si_2O_6(CO_3)(OH)_2$ where the substitution involves also the tilleyite-type module.

ACKNOWLEDGMENTS

The contribution of V.T. Dubinchuk (Russian Institute of Mineral Rough Materials, VIMS) with the electron micro-diffraction investigation is gratefully acknowledged. This work was financially supported by the Russian Foundation for Basic Research (RFBR), Project 08-05-00181a, and by MIUR (Ministero dell'Istruzione, dell'Università e della Ricerca) through a grant to the national project "Compositional and structural complexity in minerals (crystal chemistry, microstructures, modularity, modulation): analysis and applications."

REFERENCES CITED

Basso, R., Lucchetti, G., Palenzona, A., and Zefiro, L. (1995) Haradaite from the Gambatesa mine, eastern Liguria. Neues Jahrbuch für Mineralogie, Monatshefte, 1995, 281–288.

Belokoneva, E.L. (2005) Borate crystal chemistry in terms of the extended OD theory: Topology and symmetry analysis. Crystallography Reviews, 11, 151–198.

Belokoneva, E.L., Dimitrova, O.V., Korchemkina, T.A., and Stefanovich, S.Yu. (1998) $Pb_2[B_5O_9](OH)\cdot H_2O$: A new centrosymmetric modification of natural hilgardite, Hilgardite-group structures as members of the OD family. Crystallography Reports, 43, 810–819.

Belov, N.V. (1963) Crystal chemistry of large cation silicates, 162 p. Consultants Bureau, New York.

Bonaccorsi, E., Merlino S., and Kampf A. (2005) The crystal structure of tobermorite 14 Å (plombierite), a C–S–H phase. Journal of the American Ceramic Society, 88, 505–512.

Brese, N.E. and O'Keeffe, M. (1991) Bond-valence parameters for solids. Acta Crystallographica, B47, 192–197.

Dornberger-Schiff, K. (1956) On the order-disorder (OD-structures). Acta Crystallographica, 9, 593–601.

——— (1964a) Zur Strukturanalyse zweidimensional fehlgeordneter OD-Strukturen: die Strukturbestimmung des Natriumtetrametaphosphats $Na_2H_2P_4O_{12}$. Acta Crystallographica, 17, 482–491.

——— (1964b) Grundzüge einer Theorie von OD-Strukturen aus Schichten, Abhandlungen der Deutschen Akademie der Wissenschaften zu Berlin, Klasse für Chemie. Geologie und Biologie 3, 1–107.

——— (1966) Lehrgang über OD-Strukturen, 135 p. Akademie-Verlag, Berlin.

Ďurovič, S. (1997) Fundamental of the OD theory. In S. Merlino, Ed., Modular Aspects of Minerals, 1, p. 3–28. EMU Notes in Mineralogy, Eötvös University Press, Budapest.

Farrugia, L.J. (1999) WinGX suite for small-molecule single-crystal crystallography. Journal of Applied Crystallography, 32, 837–838.

Ferraris, G. and Ivaldi, G. (1988) Bond valence vs. bond length in O···O hydrogen bonds. Acta Crystallographica, B44, 341–344.

Ferraris, G., Mellini, M., and Merlino, S. (1987) Electron diffraction and electron-microscopy study of balangeroite and gageite: Crystal structures, polytypism,

and fiber texture. American Mineralogist, 72, 382–391.

Ferraris, G., Makovicky, E., and Merlino, S. (2008) Crystallography of Modular Materials, 416 p. IUCr Monographs on Crystallography 15, Oxford University Press, New York.

Ferreira, A., Ananias, D., Carlos, L.D., Morais, C.M., and Rocha, J. (2003) Novel Microporous lanthanide silicates with tobermorite-like structure. Journal of the American Chemical Society, 125, 14573–14579.

Gard, J.A. (1966) A system of nomenclature for the fibrous calcium silicates, and a study of xonotlite polytypes. Nature, 211, 1078–1079.

Grabezhev, A.I., Gmyra, V.G., and Pal'guyeva, G.V. (2004) Hydroxylellestadite metasomatites from Gumeshev skarn porphyry copper deposit, middle Urals. Doklady Earth Science, 394, 196–198.

Grabezhev, A.I., Pertsev, N.N., Zadov, A.E., Pribavkin, S.V., and Murzin, V.V. (2007) Lime-hydrosilicate metasomatites from Gumeshevsk skarn-copper-porphyric deposit Middle Urals. Petrology, 15, 552–560 (in Russian).

Grice, J.D. (2005) The structure of spurrite, tilleyite, and scawtite, and relationships to other silicate-carbonate minerals. Canadian Mineralogist, 43, 1489–1500.

Guinier, A. and 13 others (1984) Nomenclature of polytype structures. Report of the International Union of Crystallography *Ad hoc* Committee on the Nomenclature of Disordered, Modulated and Polytype Structures. Acta Crystallographica, A40, 399–404

Henmi, C., Kusachi, I., Kawahara, A., and Henmi, K. (1977) Fukalite, a new calcium carbonate silicate hydrate mineral. Mineralogical Journal, 8, 374–381.

Hoffmann, C. and Armbruster, T. (1997) Clinotobermorite, $Ca_5[Si_3O_8(OH)]_2{\cdot}4H_2O$–$Ca_5[Si_6O_{17}]{\cdot}5H_2O$, a natural C-S-H(I) type cement mineral: determination of the substructure. Zeitschrift für Kristallographie, 212, 864–873.

Kislov, E. (1998) Yoko-Dovyren Layered Massif, 256 p. Buryat Scientific Center Publishing House, Siberian Branch of Russian Academy of Sciences (in Russian).

Kopský, V. and Litvin, D.B. (2006) The 75 rod groups. In V. Kopsky and D.B.Litvin, Eds., International Tables for Crystallography, Vol. E, p. 37–217. Kluwer Academic Publishers, Dordrecht.

Liebau, F. (1956) Bemerkungen zur Systematik der Kristallstrukturen von Silikaten mit hochkondensierten Anionen. Zeitschrift für Physikalische Chemie, 206, 73–92.

——— (1985) Structural Chemistry of Silicates—Structure, Bonding, and Classification, 347 p. Springer-Verlag, Berlin.

Louisnathan, S.J. and Smith, J.V. (1970) Crystal structure of tilleyite: Refinement and coordination. Zeitschrift für Kristallographie, 132 , 288–306.

Merlino, S. (1997) OD approach in minerals: examples and applications. In S. Merlino, Ed., Eötvös Modular Aspects of Minerals, 1, p. 29–54. EMU Notes in Mineralogy, University Press, Budapest.

Merlino, S., Bonaccorsi, E., and Armbruster, T. (1999) Tobermorites: Their real structure and order-disorder (OD) character. American Mineralogist, 84, 1613–1621.

——— (2000) The real structures of clinotobermorite and tobermorite 9Å: OD character, polytypes, and structural relationships. European Journal of Mineralogy, 12, 411–429.

——— (2001) The real structure of tobermorite 11 Å: Normal and anomalous forms, OD character and polytypic modifications. European Journal of Mineralogy, 13, 577–590.

Merlino, S., Bonaccorsi, E., Merlini, M., Marchetti, F., and Garra, W. (2008) Tobermorite 11Å and its synthetic counterparts: structural relationships and thermal behaviour. In S. Krivovichev, Ed., Minerals as Advanced Materials I, p. 37–44. Springer-Verlag, Berlin.

Mizota, T., Komatsu, M., and Chihara, K. (1983) A refinement of the crystal structure of ohmilite, $Sr_3(Ti,Fe^{3+})(O,OH)(Si_2O_6)_2{\cdot}2–3H_2O$. American Mineralogist, 68, 811–817.

Otwinowski, Z. and Minor, W. (1997) Processing of X-ray diffraction data collected in oscillation mode. In C.W. Carter Jr. and R.M. Sweet, Eds., Methods in Enzymology, Volume 276: Macromolecular Crystallography, part A, p. 307–326. Academic Press, New York.

Pertsev, N.N., Konnikov, E.G., Kislov, E., Orsoev, D.A., and Nekrasov, A.N. (2003) Merwinite-facies magnesian skarns in xenoliths from dunite of the Dovyren layered intrusion. Petrologiya, 11, 464–475 (in Russian).

Plaisier, J.R., IJdo, D.J.W., de Mello Denega, C., and Blasse, G. (1995) Structure and luminescence of barium uranium disilicate ($BaUO_2Si_20_6$). Chemistry of Materials, 7, 738–743.

Rastvetaeva, R.K., Pushcharovskii, D.Yu., Konev, A.A., and Evsyunin, V.G. (1997) Crystal structure of K-containing batisite. Crystallography Reports, 42, 770–773.

Rastvetaeva, R.K., Bolotina, N.B., Zadov, A.E., and Chukanov, N.V. (2005) Crystal structure of fukalite dimorph $Ca_4(Si_2O_6)(CO_3)(OH)_2$ from the Gumeshevsk deposit, the Urals, Doklady. Earth Science, 405, 1347–1351.

Sheldrick, S. (1997) SHELX-97. Programs for crystal structure determination and refinement, Institut für Anorganische Chemie, University of Göttingen, Germany.

Takéuchi, Y. and Joswig W. (1967) The structure of haradaite and a note on the Si-O bond lengths in silicates. Mineralogical Journal (Japan), 5, 98–123.

Zadov, A.E. and Pertsev, N.N. (2005) Calc-hydrosilicates of apocarbonate xenoliths in Dovyren massif. In Proceedings of the International Conference, Ultrabasite-basite Complex of Folded Precambrian Regions, p. 80–83. Buryat Scientific Center Publishing House, Siberian Branch of Russian Academy of Sciences (in Russian).

Manuscript received July 1, 2008
Manuscript accepted October 29, 2008
Manuscript handled by Artem Oganov